

# On the ability of Moho reflections to affect the ground motion in northeastern Italy: a case study of the 2012 Emilia seismic sequence

M. Sugan · A. Vuan

Received: 24 April 2013 / Accepted: 24 November 2013 / Published online: 19 December 2013  
© The Author(s) 2013. This article is published with open access at Springerlink.com

**Abstract** It has been observed that post-critically reflected S-waves and multiples from the Moho discontinuity could play a relevant role on the ground motion due to medium to strong size earthquakes away from the source. Although some studies investigated the correlation between the Moho reflections amplitudes and the damage in the far field, little attention was given to the frequency content of these specific phases and their scaling with magnitude. The 2012 Emilia seismic sequence in northern Italy, recorded by velocimetric and accelerometric networks, is here exploited to investigate Moho reflections and multiples (SmSM). A single station method for group velocity-period estimation, based on the multiple filter technique, is applied to strong motion data to detect SmSM. Amplitude and frequency scaling with magnitude is defined for earthquakes from  $M_w = 3.9$  to  $M_w = 5.9$ . Finally, the ability of SmSM to affect the ground motion for a maximum credible earthquake within the Po plain is investigated by extrapolating observed engineering parameters. Data analysis shows that high amplitude SmSM can be recognized within the Po plain, and at the boundaries between the Po plain and the Alpine chain, at epicentral distances larger than 80 km, in the period range from 0.25 to 3 s and in the group velocity window from about 2.6 to 3.2 km/s. 5 % damped pseudo-spectral accelerations at different periods (0.3, 1.0 and 2.0 s), and Housner intensities, are obtained from data characterized by large amplitude SmSM. A scaling relationship for both pseudo-spectral accelerations and Housner intensities is found for the earthquakes of the 2012 Emilia seismic sequence.  $I_{MCS}$  from VII to VIII is estimated, as a result of SmSM amplitude enhancement, at about 100 km for a maximum credible earthquake ( $M_w = 6.7$ ) in the Po plain, showing that moderate to high damage could be caused by these specific phases.

---

M. Sugan (✉)

Istituto Nazionale di Oceanografia e di Geofisica Sperimentale, OGS, Sezione Centro Ricerche Sismologiche, Via Treviso 55, 33100 Cussignacco, Udine, Italy  
e-mail: msugan@inogs.it

A. Vuan

Istituto Nazionale di Oceanografia e di Geofisica Sperimentale, OGS, Sezione Centro Ricerche Sismologiche, Borgo Grotta Gigante 42c, 34010 Sgonico, Trieste, Italy  
e-mail: avuan@inogs.it

**Keywords** Moho reflections · 2012 Emilia seismic sequence · Multi filter technique · Far field · Strong motion · Macroseismic intensity · Housner intensity · Pseudo-spectral acceleration

## 1 Introduction

The Emilia seismic sequence of moderate-sized earthquakes started on May 2012, in northern Italy (Po plain), where a thick (>2 km) sedimentary alluvial deposits cover the external active fronts of the Apennine belt (e.g. [Pieri and Groppi 1981](#)). Two major events shook the region on May 20 (Mw 6.1, at 02:03 UTC) and May 29 (Mw 5.9, at 07:00 UTC). About 30 earthquakes of magnitude above 4.0 were recorded in the first month of the sequence (<sup>©</sup> ISIDe Working Group (INGV 2010), last accessed December 2012). Moment tensor (MT) solutions shows predominantly reverse faulting, with a variable component of strike-slip ([Pondrelli et al. 2012](#); [Saraò and Peruzza 2012](#)), in agreement with the structural setting of the area, characterized by north verging blind thrust faulting ([Boccaletti et al. 2004](#)).

In the near field, the strong ground motion recorded during the sequence, together with the duration of the perturbation, caused casualties and severe damage to civil and industrial structures, as well as to the historical and cultural heritage of the area ([Piccinini et al. 2012](#)). Damage and seismic effects were also found far from the source at epicentral distances greater than 50 km ([Galli et al. 2012](#)). According to the web-based macroseismic survey, by Istituto Nazionale di Geofisica e Vulcanologia (INGV) main shocks were felt in a large portion of northern Italy, up to 200 km (INGV, <http://www.haisentitoilterremoto.it>, last accessed September 2012). Such a long-distance effect has been observed elsewhere by [Liu and Tsai \(2009\)](#) and [Eberhart-Phillips et al. \(2010\)](#), suggesting large amplitude SmSM as the cause for the damage and strong perception.

Previously, in central California, [Bakun and Joyner \(1984\)](#) found that the large positive residuals in  $M_L$  at distances between 75 and 125 km, could be a result of Moho reflections. Few years later, [Burger et al. \(1987\)](#) published the attenuation relations of eastern North America, which showed amplitudes in the distance range of 60–150 km to be higher than those at smaller and greater distances.

[Bragato et al. \(2011\)](#) pointed out how currently available peak ground motion predictive equations largely underestimate the level of shaking in northeastern Italy, showing that the Moho reflection effect is maximized at hypocentral distances between 90 and 150 km.

Recently, [Sugan and Vuan \(2012\)](#) investigated the amplitude and frequency content of SmSM, using a time-frequency analysis of accelerometric recordings, and evaluated the transfer functions due to soft soils for SmSM considering a medium-sized inland Japanese earthquake, where borehole and surface data were available. They showed that the spectral amplitude enhancement for these specific phases is well correlated with National Earthquake Hazard Reduction Program (NEHRP) soil classification; the average transfer functions between A + B and C sites, and C and D sites are both enhanced by a factor of about 2.

The Po plain region is only recently instrumented by strong motion stations, and for the first time the 2012 Emilia seismic sequence gives an opportunity to study wave propagation and SmSM generated and recorded within the deep basin. The method described in [Sugan and Vuan \(2012\)](#) is here applied to some earthquakes of the seismic sequence to identify the SmSM amplitudes and their scaling with magnitude within a specific frequency range. SmSM amplitude enhancement was analysed in term of peak ground acceleration (PGA) by [Bragato et al. \(2011\)](#) using earthquakes at hypocentral depths of about 20 km, localized at the edge of the Po plain, along the Apenninic chain. The case study of the 2012 Emilia

seismic sequence is of particular interest to understand if amplitude enhancement at specific distances due to SmSM can be observed also for earthquakes located within the Po plain and at shallower depth than those previously investigated in [Bragato et al. \(2011\)](#).

The method adopted does not require any manual picking of the waveforms, or need an a priori well-known structural model. Nevertheless, we compute some synthetic seismograms using a simple 1D velocity model ([Vuan et al. 2011](#)), to verify the consistency between synthetic and observed SmSM travel time arrivals. The computation strengthens the recognition of SmSM, performed in the frequency-time domain on the basis of multiple filter technique (MFT).

For evaluating if a far strong earthquake characterized by large amplitude SmSM can affect the ground motion, we perform an estimation of the spectral accelerations (SAs) and Housner intensities (SI) of observed data in the moment magnitude range from  $M_w = 3.9$  to  $M_w = 5.9$ . Macroseismic intensities at about 100 km from the source are then extrapolated from SAs and SI parameters, assuming a maximum credible earthquake, in the Po plain (northern Italy).

## 2 Multiple filter technique applied to the 2012 Emilia seismic sequence

The method described in [Sugan and Vuan \(2012\)](#) is applied to the dataset recorded in the northern Italy during the 2012 Emilia seismic sequence, to identify the SmSM amplitude enhancement. The procedure uses a single station method for group velocity-period estimation, based on the MFT. A comb of narrow band filters with varying central frequency is applied to the signal. Instantaneous spectral amplitudes are then displayed in terms of time and frequency (group velocity and period). MFT analysis allows the recognition of different seismic phases (surface waves, body waves, high frequency scattered waves) in the group velocity-period domain, where SmSM can be described as a superposition of higher modes of surface waves ([Oliver and Ewing 1957, 1958](#)).

MFT is performed using the code developed by [Herrmann \(2013\)](#) and computed in the group velocity and period range from 0.1 to 7 km/s and 0.1–30 s, respectively. Further details on the SmSM detection technique can be found in [Sugan and Vuan \(2012\)](#), where the method is validated by using synthetic seismograms and observations.

The 2012 Emilia seismic events that have been selected in this study are listed in [Table 1](#). The earthquakes are variable in magnitude but are consistent in terms of focal mechanism solutions (e.g. [Saraò and Peruzza 2012](#)) and depths, allowing the analysis to avoid possible significant differences in the seismic source radiation pattern. The selected earthquakes are clustered near the 29 May ( $M_w$  5.9, at 07:00 UTC) event, and all have hypocentral depths above 11 km (<sup>©</sup> ISIDE Working Group (INGV 2010), last accessed December 2012).

The main shock that occurred on 20 May, 2012 ( $M_w$  6.1, at 02:03 UTC) has not been accounted for the analysis, since it clearly shows a complex pattern of rupture, with at least two separate pulses ([Piccinini et al. 2012](#)), whose combination could bias our analysis.

Earthquake locations and seismic stations are shown in [Fig. 1](#), together with the location of the seismic section A–A', used in this study to evaluate SmSM travel time arrivals.

We use velocimetric data from INGV (Istituto Nazionale di Geofisica e Vulcanologia) and OGS (Istituto Nazionale di Oceanografia e Geofisica Sperimentale) and accelerometric data from INGV ([Massa et al. 2012](#)), located in the distance range from 0 to about 250 km from the epicentral area (see [Sect. 6](#)).

All the velocimetric waveforms are corrected for the instrumental responses and then differentiated to obtain accelerograms on which the analysis is performed. Horizontal com-

**Table 1** Earthquakes used in this study

List of the analyzed earthquakes											
ID	Date yyyy/mm/dd Time (UTC)	Lat. (N)	Long. (E)	Dep. (km)	Ml	Strike (°)	Dip (°)	Rake (°)	Mo (Nm)	Mt Dep. (km)	Mw
1	2012/05/20 03:02:50	44.860	11.095	10.0	4.9	279 (98)	64 (26)	90 (89)	3.70e+16	8	5.0
2	2012/05/23 21:41:18	44.868	11.251	4.8	4.3	271 (105)	57 (33)	83 (101)	1.47e+14	6	4.1
3	2012/05/29 07:00:303	44.851	11.086	10.2	5.8	274 (97)	64 (26)	89 (93)	7.66e+17	6	5.9
4	2012/05/29 08:25:51	44.901	10.943	3.2	4.5	279 (97)	68 (22)	91 (88)	9.41e+15	6	4.6
5	2012/05/29 10:55:57	44.888	11.008	6.8	5.3	269 (105)	65 (26)	83 (105)	2.28e+17	6	5.5
6	2012/05/31 19:04:04	44.891	10.980	8.7	4.2	97 (280)	49 (41)	92 (–88)	7.11e+14	10	3.9

Locations are taken from ISIDE (© ISIDE Working Group (INGV 2010), Italian Seismological Instrumental and parametric database), MT solutions are taken from [Saraò and Peruzza \(2012\)](#)

ponents are rotated to provide radial and transverse components. The rotation is performed to better identify SmSM on MFT diagrams as superposition of Love or Rayleigh higher modes (transverse and radial components, respectively). Depending on the radiation pattern the energy is differently split on the two components. Figure 2 shows an example of the MFT diagrams obtained for the transverse component of two earthquakes, recorded by SANR accelerometric station (see Fig. 1 for location), at a distance of about 95–97 km. The transverse component in Fig. 2 has spectral amplitude values greater than the radial component. The largest SmSM spectral amplitudes are clearly found at group velocities of about 3 km/s, while low amplitude surface waves are found at lower group velocities (about 2 km/s) and longer periods. Surface waves amplitudes can enhance at a disadvantage of SmSM amplitudes by using velocities or displacements instead of accelerations in the analysis (see [Sugan and Vuan 2012](#)).

The existence of the SmSM domain can be detected predominantly in the azimuth range  $0^\circ$ – $90^\circ$ , in agreement with [Bragato et al. \(2011\)](#) for northeastern Italy. Propagation of these kind of waves seems to be more efficient than elsewhere. Lg waves, at the same, propagate efficiently within the Po plain that is included in the Adriatic plate ([Mele et al. 1997](#)). Both SmSM and Lg waves can be interpreted as a superposition of higher modes of surface waves, even if Lg are found on longer source–receiver paths than SmSM.

Single station MFTs are used trying to highlight the distance–period window where SmSM are relevant. Figure 3 shows the corresponding normalized spectral amplitude for all the stations in the northeastern sector (source–receiver azimuth from  $0^\circ$  to  $90^\circ$ ), as a function of period versus distance in the 0.1–5 s period range, for the two earthquakes that occurred on May 20 at 03:02:50 (Mw 5.0), and on May 29 at 07:00 UTC (Mw 5.9). These two events are consistent in MT solutions and epicentral parameters, even if they are slightly different in MT focal depth (see Table 1).

A large amplitude SmSM domain can be recognized from about 80 to 160 km, at periods up to 3 and 2 s for the Mw 5.9 and Mw 5.0 events, respectively. The enhancement of amplitudes

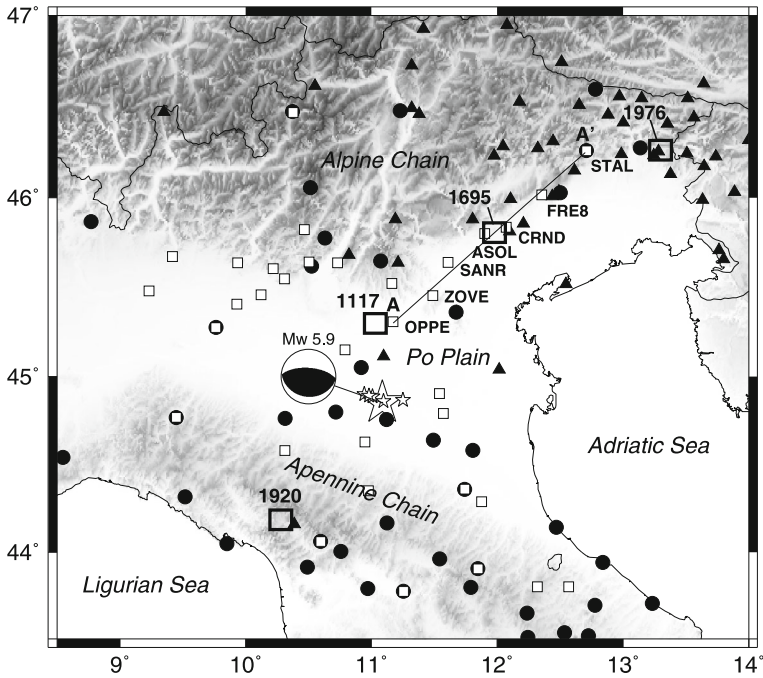


**Fig. 1** Location map of the earthquakes shown in Table 1 (white stars) and of the seismic stations used in this study. OGS seismic stations (black triangles), INGV velocimetric seismic stations (black circles) and INGV accelerometric seismic stations (white squares) (see Sect. 6). Seismic section A–A' is located at the boundaries between the Po plain and Alpine chain. The epicenters of the historical earthquakes occurred in 1117, 1695, 1920 and 1976 are shown (see text for details). The MT solution of the strongest event (ID 3 in Table 1) is mapped (Saraò and Peruzza 2012). Map created using Wessel and Smith (1991)

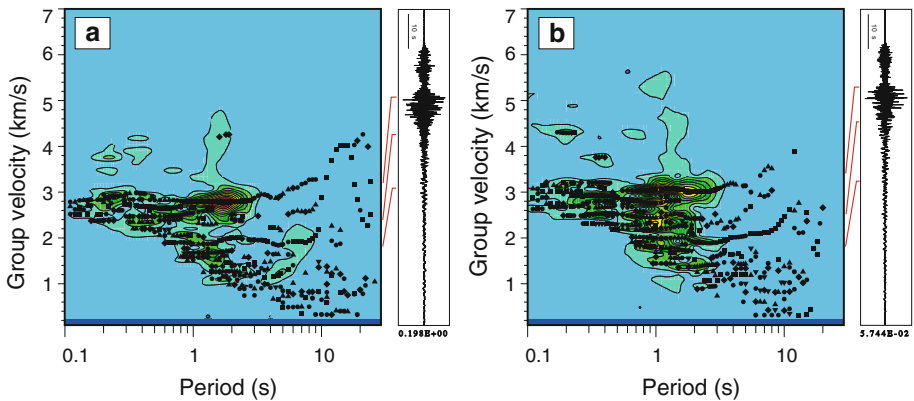


**Fig. 2** MFT analysis on SANR accelerometric INGV seismic station (transverse components are shown). **a** Mw 5.9 event (ID 3 in Table 1); **b** Mw 5.0 event (ID 1 in Table 1). Color scale is in dB; red represents 100 dB. Dotted black symbols show the maximum coherence of the signal on MFT diagrams. The waveform of the analyzed signal and the maximum amplitude value are shown

at specific distances has been associated with an efficient propagation of SmSM in this portion of the crust where the Moho discontinuity shows a variable depth range from 25 to 35 km (Finetti 2005) and an evident impedance contrast exists between the upper crust and the Moho.

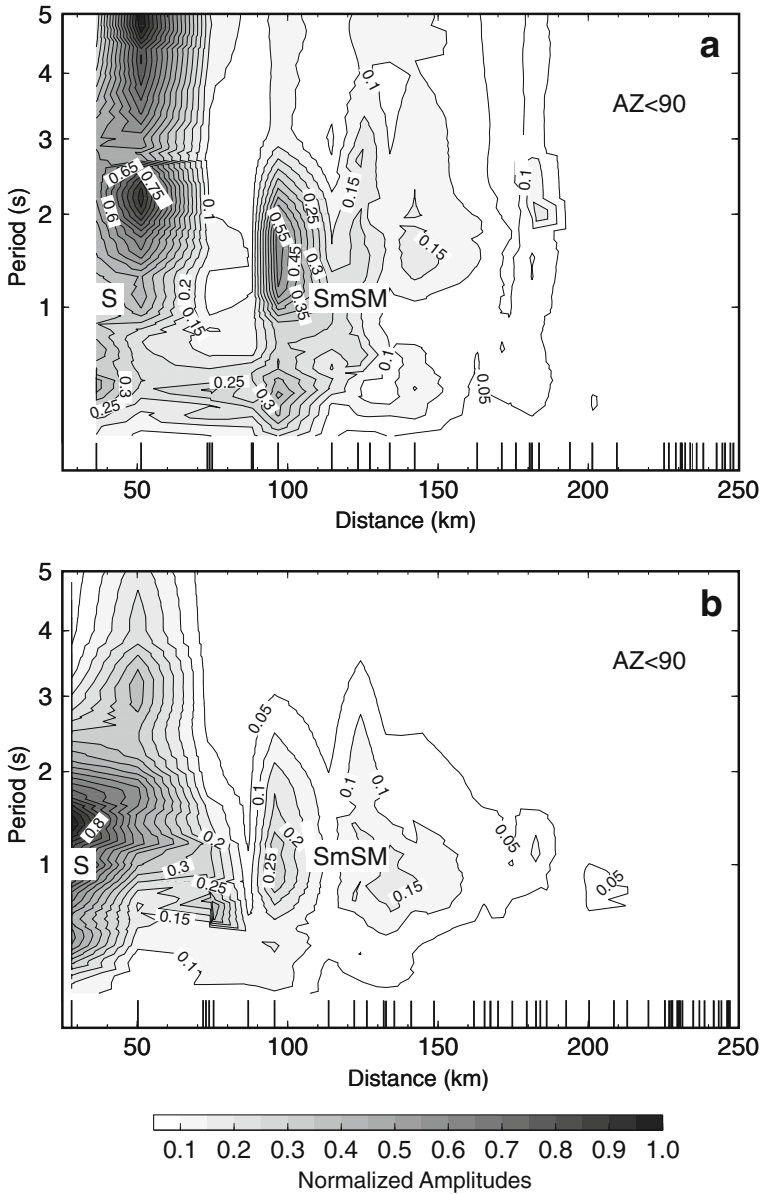


**Fig. 3** Normalized spectral amplitude as a function of distance and period for the radial and transverse components together. **a** 29 May, Mw 5.9 (at 07:00 UTC), analysis in the azimuth  $0^\circ-90^\circ$ ; **b** 20 May, Mw 5.0 (at 03:02 UTC), analysis in the azimuth  $0^\circ-90^\circ$ . S represents upgoing S waves and SmSM represents the critical and postcritical reflected SmS. Each black bar at the bottom of each graph represents a seismic station at that specific distance

In general, the SmSM amplitudes are enhanced especially when earthquakes occur close to the Moho boundary, therefore for earthquakes deeper than those of the 2012 Emilia seismic sequence SmSM amplitudes can be even larger.

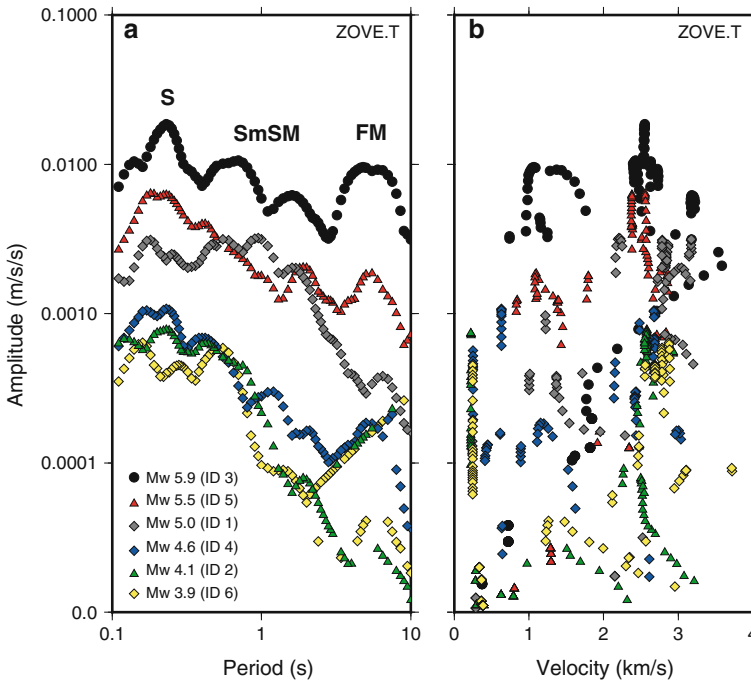


**Fig. 4** ZOVE (accelerometric INGV seismic station) spectral amplitude-period graph (a), and spectral amplitude-velocity graph (b) for earthquake in Table 1, transverse (T) component. See Fig. 1 for station location

### 3 Moho reflections at single stations

The enhancement of SmSM at specific distances is controlled by the crustal thickness, earthquake depth, and source radiation pattern, and clearly shows regional variations (e.g. Somerville and Yoshimura 1990; Furumura 2001; Liu and Tsai 2009; Eberhart-Phillips et al. 2010).

In the azimuthal range from 0° to 90° in the northeastern Italy, ZOVE, SANR and ASOL, located at distances of about 75, 95 and 123 km respectively are characterized by the largest amplitude SmSM.

For each period (from 0.1 to 30 s) the maximum MFT amplitude (and the corresponding group velocity) is taken and the spectral amplitude-period and spectral amplitude-velocity values are visualized for each station and each seismic event of Table 1 (Figs. 4, 5, 6). The transverse component is shown since it has spectral amplitude values higher than the radial one.

The MFT spectral amplitude-period graphs (see Figs. 4a, 5a, 6a) clearly shows almost three distinct domains: (1) the first is related to the arrival of S-waves (periods lower than 1 s); (2) the second to the arrival of SmSM (periods up to 2–3 s); and (3) the third to the long period surface waves (periods above 3 s and apparent velocity lower than 2.3 km/s). From ZOVE (at a distance of about 75 km) to ASOL (at a distance of about 123 km), the energy distribution varies (Figs. 4, 5, 6), and the maximum amplitude pick shifts from S-wave at ZOVE station to SmSM phases at SANR station, located at about 95 km (Fig. 5).

The highest SmSM amplitude is recorded by SANR station. This station is located along the seismic section A–A', in an area characterized by an efficient SmSM propagation, at

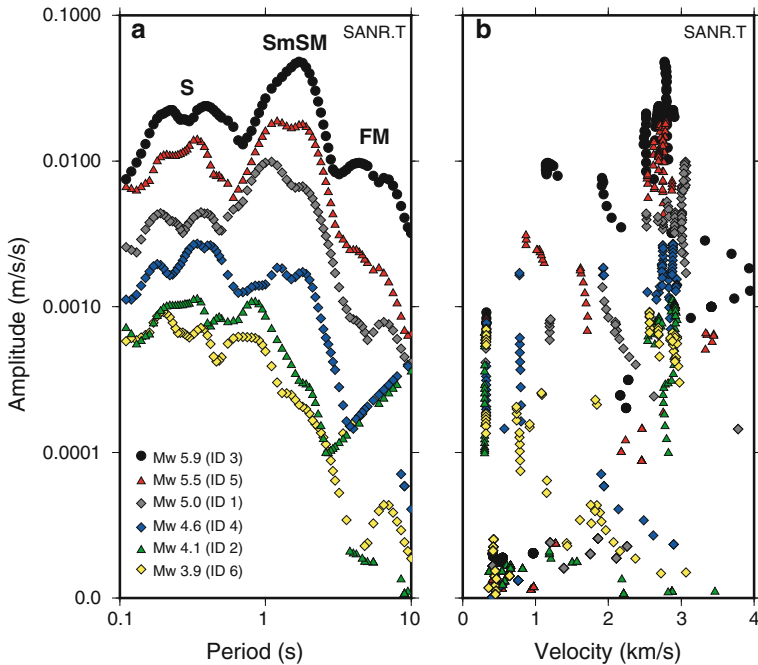


**Fig. 5** SANR (accelerometric INGV seismic station) spectral amplitude-period graph (a), and spectral amplitude-velocity graph (b), for earthquake in Table 1, transverse (T) component. See Fig. 1 for station location

the boundary between the Po plain and the Alpine chain. Site class of SANR according to Eurocode8 (EC8) is C.

By analyzing MFT diagrams of SANR station we can observe that as the magnitude increases, the pick amplitude shifts towards longer periods, while surface waves amplitude also enhances in the range from 3 to 10 s (see Fig. 5a). Lower frequencies are normally associated with larger earthquakes. Similar findings are, generally, common to all the stations located along the A–A' section. Figure 5b shows the SANR spectral amplitude-velocity domain dataset. Large amplitude SmSM have group velocities from 2.6 to 3.1 km/s. The shift observed in the apparent velocity range between the Mw 5.9 and the Mw 5.0 events, could be related both to uncertainties in defining the origin time of the events, and/or to possible slight differences in hypocentral depths among the events. A common depth of about 10 km is reported in the preliminary locations (<sup>©</sup> ISIDE Working Group (INGV 2010), last accessed December 2012), while moment tensor available solutions indicate a deeper hypocenter for the Mw 5.0 event (see Table 1) respect to the other events (Pondrelli et al. 2012; Sarà and Peruzza 2012). However, group velocities lower than 2.3 km/s, that can be associated with surface waves amplitudes, show a consistent frequency range for the Mw 5.9 and Mw 5.0 events (Fig. 5b). Reflected waves that are characterized by a sub-vertical propagation, are more sensitive to lateral heterogeneities and are probably more influenced by different hypocentral source depth, than surface waves travelling mainly in the horizontal plane. This could explain the velocity shift observed for SmSM for the Mw 5.9 and the Mw 5.0 events.

The spectral amplitude-period relationships, for the two events of Mw 5.9 and 5.0 in Table 1, are analyzed along the A–A' seismic section for the transverse component. In Fig. 7 the maximum spectral amplitude is reached at a distance of about 50 km (OPPE), and is



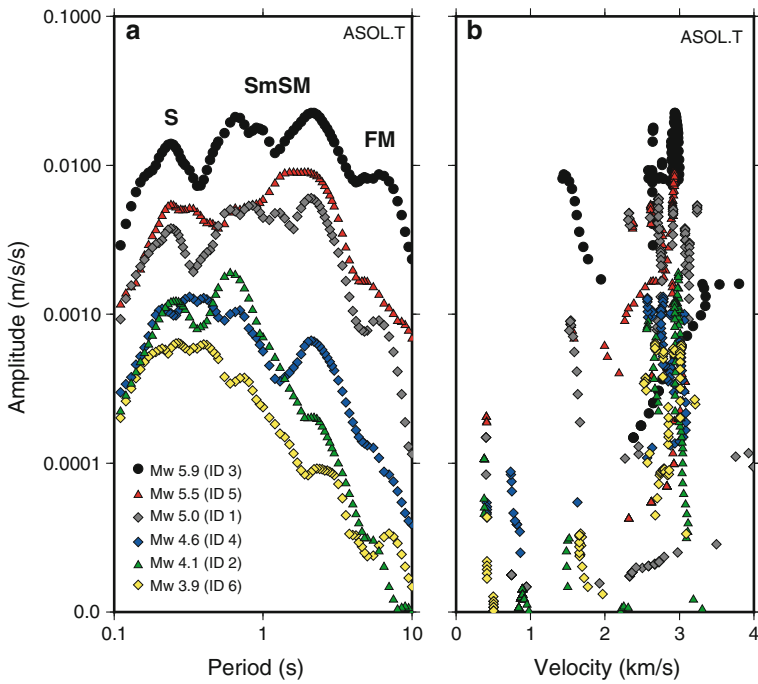


**Fig. 6** ASOL (accelerometric INGV seismic station) spectral amplitude-period graph (a), and spectral amplitude-velocity graph (b), for earthquake in Table 1, transverse (T) component. See Fig. 1 for station location

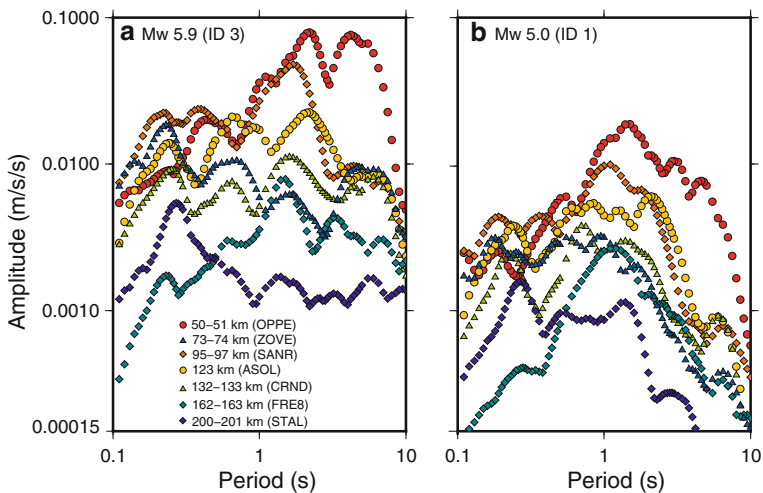


**Fig. 7** Spectral amplitude-period graphs for the events that occurred (a) on May 29, Mw 5.9 (at 07:00 UTC) and (b) on May 20, Mw 5.0 (at 03:02 UTC). See Fig. 1 for earthquakes and station locations. The transverse components are shown

related to low velocity surface waves. SANR station (EC8 class C site) clearly recorded higher amplitudes than the nearer ZOVE station (EC8 class A site); in this case, amplitude values are related both to SmSM (see Fig. 5) and local site effects.

**Table 2** Velocity model (Vuan et al. 2011)

Velocity model				
Thickness (km)	$V_P$ (km/s)	$V_S$ (km/s)	$Q_P$	$Q_S$
0.5	1.5	0.6	20	10
0.5	2	1.2	200	100
0.5	2.42	1.4	200	100
1.5	3.9	2.25	600	300
2	4.75	2.75	1000	500
15	6.05	3.5	1000	500
10	6.8	3.93	1000	500
20	7.7	4.41	1000	500
50	7.7	4.31	1000	500
50	7.7	4.21	1000	500
50	7.7	4.31	1000	500
Half-space	7.79	4.41	1000	500

To evaluate travel time arrivals between synthetic and observed group velocities, we perform some numerical simulations using the Wavenumber Integration Method (WIM; Herrmann 2013). WIM computes synthetic seismograms for a point source described by its focal mechanism, seismic moment, and depth, solving the full-wave equation in anelastic media, with an horizontally layered structure. We adopted the 1-D crustal model proposed by Vuan et al. (2011), which includes 7 crustal layers and Q factors, and the Moho at 30 km (Table 2). Furthermore, we used the focal mechanism of the Mw 5.0 event, so that the point source approximation is still acceptable. The strike, dip and slip angles of the two nodal planes are those obtained by Sarò and Peruzza (2012): 279°, 64° and 90° for the first plane; 98°, 26° and 89° for the second plane. We set the source depth at 10 km, and assume a source time function of 0.8 s, to compute synthetic accelerograms for frequencies up to 4 Hz. Receivers are placed at the surface, corresponding to recorded data along the A–A' seismic section, at epicentral distances from 50 to 200 km. Figure 8 shows the comparison of synthetic and observed accelerations for the radial and transverse components. The SmSM observed travel time arrivals are characterized by an apparent velocity in the range from 2.6 to 3.2 km/s (dashed lines in Fig. 8) and are consistent with synthetic SmSM travel times. The match between waveforms can be considered satisfactory, even in terms of Q crustal structure.

#### 4 Can SmS reflections and multiples cause damage in and around the Po plain?

The maximum expected magnitude in northern Italy and surroundings can be defined from “Catalogo Parametrico dei Terremoti Italiani (CPTI)” (Rovida et al. 2011) and by the Database of Individual Seismogenic Sources (DISS) 3.1.1 (DISS Working Group 2010; Basili et al. 2008). According to the seismogenic zonation of Italy, and the historical seismic events selected in the Italian macroseismic catalogs (e.g., Stucchi et al. 2007; Locati et al. 2011), the stronger historical events in the surrounding of the 2012 Emilia seismic sequence are: (1) the 1117 Mw = 6.7 Veronese earthquake; (2) the 1695 Mw = 6.5 Asolo earthquake; and (3) the 1920 Mw = 6.5 Garfagnana earthquake (Fig. 1). In particular, the strongest event is associated with the debated source of the January 3, 1117 earthquake; that has been hypothesized to be either a segment of the Eastern South-Alpine chain on the Veneto plain

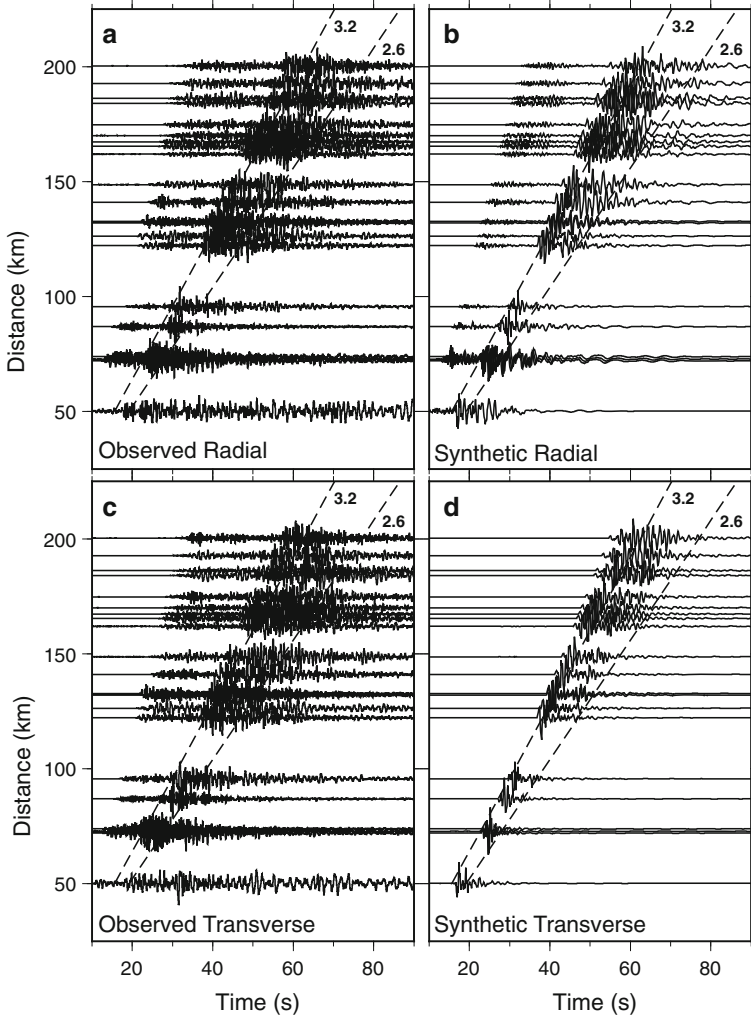


**Fig. 8** Observed (a, c) and synthetic (b, d) accelerations for the radial and transverse components along the section A–A' in Fig. 1. The apparent velocities of 2.6 and 3.2 km/s are represented by dashed lines. SmSM phases are generally included in the apparent velocity fan. The same band pass filter from 0.2 to 4 Hz is applied

(shown in Fig. 1), east of the Lessini chain (Galadini et al. 2005), or a blind thrust of the northern Apennine chain near Cremona (Galli 2005).

Using data from SANR accelerometric station and for the events in Table 1 we estimate the 5% damped SAs at the periods of 0.3, 1.0 and 2.0 s, and SI in the range from 0.1 to 2.5 s (Housner 1952).

SAs can be related to the MCS macroseismic intensity ( $I_{MCS}$ ) using the available period dependent regression (Faenza and Michelini 2011) while SI has been evaluated since it has been recently considered a very effective parameter to correlate the severity of seismic events with building structural damage (Pergalani et al. 1999; Masi et al. 2010; Chiazzi et al. 2012). For SI both  $I_{MCS}$  and European Macroseismic Scale—EMS98 intensity ( $I_{EMS}$ , Grünthal 1998) are evaluated.

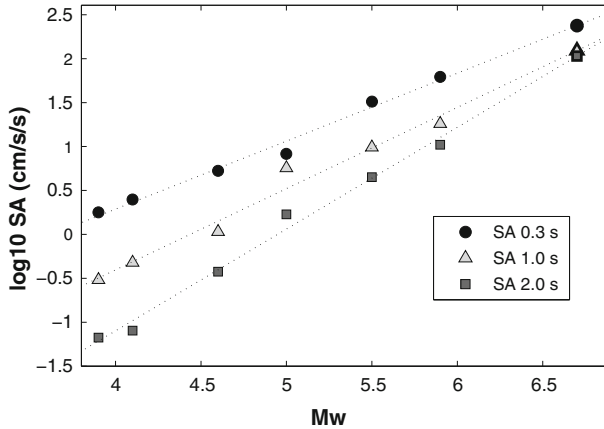


**Fig. 9** SANR SAs (0.3, 1 and 2 s) as a function of Mw. The values at Mw 6.7 are extrapolated using a linear fit

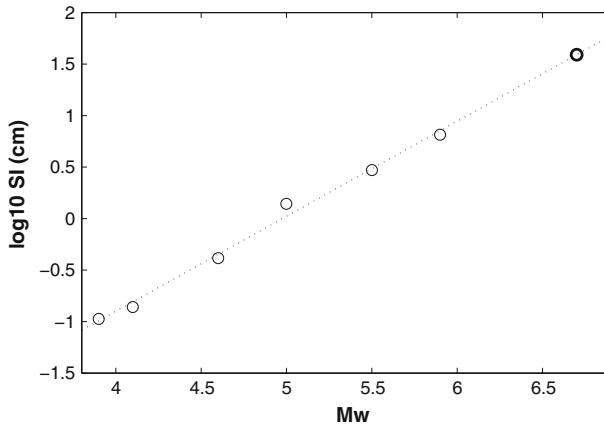


**Fig. 10** SANR SI as a function of Mw. The values at Mw 6.7 are extrapolated using a linear fit

A linear fitting is tried to extrapolate SAs and SI for an earthquake of  $M_w = 6.7$ , the maximum expected magnitude (Figs. 9, 10). In Table 3 we list the SAs values observed for  $M_w = 5.9$  and the extrapolated ones for the maximum credible earthquake ( $M_w = 6.7$ ). MCS intensity is determined using the regressions developed by Faenza and Michelini (2011), considering the maximum SA among the two horizontal components. The MCS values we find for the  $M_w = 5.9$  are 1° higher than those provided by the macroseismic study of the 2012 Emilia sequence by Galli et al. (2012).  $I_{MCS} = VII$  and  $I_{MCS} = VIII$  can be obtained at periods of 1 and 2 s, respectively, for a possible  $M_w = 6.7$  earthquake.

In addition, we use the regressions between  $I_{MCS}$  and SI (Koliopoulos et al. 1998) and  $I_{EMS}$  and SI (Chiauzzi et al. 2012). The linear trend between Mw and SI is shown in Fig. 10, while in Table 4 we list the SI values observed and extrapolated for  $M_w = 5.9$  and  $M_w = 6.7$ . SI values obtained for the  $M_w 5.9$  fit the  $I_{MCS}$  provided by Galli et al. (2012). Both regressions in Table 4 pointed out a MCS and EMS98 intensity of about VII for a  $M_w = 6.7$ , indicating that moderate to heavy damage from a strong earthquake can be expected at some critical distances in northeastern Italy.

**Table 3** SAs values obtained for the Mw 5.9 (SANR station and event ID 3 in Table 1) and extrapolated for a Mw 6.7 earthquake (see Fig. 9) and the corresponding value of  $I_{MCS}$  calculated using the regression of Faenza and Michelini (2011)

SAs– $I_{MCS}$					
Mw	SAs (s)	log10 SAs (cm/s/s)	$I_{MCS}$		$\sigma$ ( $I_{MCS}$ )
5.9	0.3	1.79	5.66	VI	0.53
	1.0	1.26	5.70	VI	0.36
	2.0	1.02	6.35	VI	0.29
6.7	0.3	2.38	7.12	VII	0.53
	1.0	2.09	7.40	VII	0.36
	2.0	2.03	8.37	VIII	0.29

**Table 4** SI values obtained for the Mw 5.9 (SANR station and event ID 3 in Table 1) and extrapolated for a Mw 6.7 earthquake (see Fig. 10) and the corresponding value of  $I_{MCS}$  calculated using the regression of Koliopoulos et al. (1998) and  $I_{EMS}$  using Chiauuzzi et al. (2012)

SI– $I_{MCS}$ and SI– $I_{EMS}$							
Mw	SI			$I_{MCS}$		$I_{EMS}$	
	cm	ln (cm)	log10 (cm)	Koliopoulos et al. (1998)		Chiauuzzi et al. (2012)	
5.9	6.53	1.88	0.815	4.77	V	5.28	V
6.7	38.90	3.66	1.59	7.00	VII	6.65	VII

Generally, the ability or not of some engineering parameters to correlate with MCS intensity has to be evaluated specifying the spectral range. Riddel (2007) showed that acceleration related indices are the best for rigid systems, velocity-related indices are better for intermediate systems, and displacement-related indices are better for flexible systems. Rigid, intermediate, and flexible systems can be characterized by periods of about 0.2, 1, and 5 s, respectively (Riddel 2007). Since our study focuses on SmSM, propagating far from the source, with maximum spectral amplitudes in the period range from 0.25 to 3 s, it is not surprising that MCS intensity is better correlated with SI than period dependent SA. Other studies (Decanini et al. 2002; Masi et al. 2010) have demonstrated that SI can be an effective parameter to correlate the severity of seismic motions to structural damage, particularly in cases of existing non-ductile reinforced concrete buildings.

To have a further evidence of our results we consider the macroseismic field of the 1976 Mw = 6.5 Friuli earthquake in northeastern Italy (Fig. 1). The Italian Macroseismic Database (Locati et al. 2011) for the Friuli earthquake presents four localities at distances consistent with a possible SmSM amplitude enhancement with  $I_{MCS}$  = VI–VII in agreement with  $I_{MCS}$  values (Tables 3, 4) extrapolated from the 2012 Emilia seismic sequence. The same macroseismic catalogue shows also that  $I_{MCS}$  = VIII has been previously reached in northern Italy at an epicentral distance of about 100 km for the 1117 Mw = 6.7 Veronese earthquake, even if historical data are poorly constrained.

### 5 Discussion and conclusions

Using a previously developed and validated procedure (see Sughan and Vuan 2012), we identify and investigate the SmSM amplitude and frequency domain scaling with magnitudes (Mw from 3.9 to 5.9) observed in the northern Italy during the 2012 Emilia seismic sequence.

High amplitude SmSM reflections have been recognized at epicentral distances larger than 80 km, in the period range from 0.25 to 3 s and in the group velocity window from 2.6 to 3.2 km/s.

The SmSM propagate efficiently in the azimuth  $0^{\circ}$ – $90^{\circ}$  due to a combination of radiation pattern, crustal properties, and local effects. Analyzing the events of the same seismic sequence with consistent focal mechanisms and epicentral locations, we observe that as the magnitude increases, the SmSM pick amplitude shifts towards longer periods, while similarly, the surface wave amplitudes enhance in the period range from about 3 to 10 s.

The amplitudes of different phases (S-waves, Moho reflections and multiples, surface waves) are modulated with distance. Along a section characterized by efficient SmSM propagation, at epicentral distances from about 75 to 123 km, the maximum amplitude pick shifts from S to SmSM domain, with the largest SmSM amplitude enhancement at about 95 km (SANR station, EC8 class C site). Comparing the peak ground acceleration value (PGA), the pseudo-spectral accelerations and Housner intensity observed at SANR for the Mw 5.9 earthquake with ground motion prediction equation (Bindi et al. 2011) we find that PGA and SA (1 s) are increased by a factor of about 2–3 due to SmSM phases and a local site effect, while SI is increased by a factor of about 1.3.

The ground motion pseudo-spectral acceleration and Housner intensity scaling with magnitude at SANR station allow us to extrapolate the corresponding values for a Mw 6.7 earthquake: the maximum credible magnitude in northern Italy in the surroundings of the 2012 Emilia sequence.

The available regressions applied to some shallow earthquakes of the 2012 Emilia sequence show that an average  $I_{MCS} = VII$ – $VIII$  (moderate to high damage) can be expected at distances of about 100 km, for a Mw 6.7 earthquake at an EC8 C site.

For the same magnitude, an event characterized by even deeper focal depth could show larger SmSM amplitudes and therefore could further increase macroseismic intensities. An additional enhancement should be expected for D sites, as pointed out by [Sugan and Vuan \(2012\)](#).

## 6 Data and resources

We used data released from Istituto Nazionale di Geofisica e Vulcanologia (INGV) and Istituto Nazionale di Oceanografia e di Geofisica Sperimentale (OGS). OGS data include other Italian and international institutions: e.g. the Province of Trento (Provincia Autonoma di Trento) and Veneto Region in Italy; the Environmental Agency of the Republic of Slovenia (ARSO); and the Austrian Central Institute for Meteorology and Geodynamics (Zentralanstalt für Meteorologie und Geodynamik, ZAMG). The INGV data used in this work are available at the Web addresses <http://iside.rm.ingv.it> (<sup>©</sup> ISIDe Working Group (INGV 2010), Italian Seismological Instrumental and parametric database, last accessed September 2012) and <http://ismd.mi.ingv.it/ismd.php>.

**Acknowledgments** This research was supported by the Civil Protection of the Regione Veneto and of the Regione Autonoma Friuli Venezia Giulia. The OGS Network is supported financially by the Civil Protection of the Regione Autonoma Friuli Venezia Giulia, and Regione Veneto, and by the Geological Survey of Provincia Autonoma di Trento. We thank the technical staff of the Centro Ricerche Sismologiche (CRS-OGS) for data acquisition and processing and P.L. Bragato. This research has benefited from data provided by the Istituto Nazionale di Geofisica e Vulcanologia (INGV). We are grateful to Paolo Augliera and Marco Massa, and all the people involved in the design, development and maintenance of INGV network.

**Open Access** This article is distributed under the terms of the Creative Commons Attribution License which permits any use, distribution, and reproduction in any medium, provided the original author(s) and the source are credited.

## References

- Bakun WH, Joyner WB (1984) The ML scale in central California. *Bull Seismol Soc Am* 74(5):1827–1843
- Basili R, Valensise G, Vannoli P, Burrato P, Fracassi U, Mariano S, Tiberti MM, Boschi E (2008) The Database of Individual Seismogenic Sources (DISS), version 3: summarizing 20 years of research on Italy's earthquake geology. *Tectonophysics* 453:20–43
- Boccaletti M, Bonini M, Corti G, Gasperini P, Martelli L, Piccardi L, Tanini C, Vannucci G (2004) Carta sismotettonica della regione Emilia-Romagna. Scala 1:250000 Note illustrative. Regione Emilia-Romagna—CNR IGG, Servizio Geologico, Sismico e dei Suoli, Bologna, Italy, p 60
- Bragato PL, Sukan M, Augliera P, Massa M, Vuan A, Saraò A (2011) Moho reflection effects in the Po plain (northern Italy) observed from instrumental and intensity data. *Bull Seismol Soc Am* 101(5):2142–2152
- Burger RW, Somerville PG, Barker JS, Herrmann RB, Helmberger DV (1987) The effect of crustal structure on strong ground motion attenuation relations in eastern North America. *Bull Seismol Soc Am* 77(2):420–439
- Chiauzzi L, Masi A, Mucciarelli M, Vona M, Pacor F, Cultrera G, Gallovič F, Emolo A (2012) Building damage scenarios based on exploitation of Housner intensity derived from finite faults ground motion simulations. *Bull Earthq Eng* 10:517–545
- Decanini L, Mollaioli F, Oliveto G (2002) Structural and seismological implications of the 1997 seismic sequence in Umbria and Marche, Italy. In: Oliveto G (ed) *Innovative approaches to earthquake engineering*. WIT Press, Southampton, pp 229–323
- DISS Working Group (2010) Database of Individual Seismogenic Sources (DISS), version 3.1.1: a compilation of potential sources for earthquakes larger than M 5.5 in Italy and surrounding areas. INGV (Istituto Nazionale di Geofisica e Vulcanologia, Roma, Italy); all rights reserved, <http://diss.rm.ingv.it/diss>
- Eberhart-Phillips D, McVerry G, Reyners M (2010) Influence of the 3D distribution of Q and crustal structure on ground motions from the 2003 Mw 7.2 Fiordland, New Zealand, earthquake. *Bull Seismol Soc Am* 100(3):1225–1240
- Faenza L, Michelini A (2011) Regression analysis of MCS intensity and ground motion spectral accelerations (SAs) in Italy. *Geophys J Int* 186:1415–1430
- Finetti I (2005) Crustal tectono-stratigraphic sections across the western and eastern Alps from ECORS-CROP and transalp seismic data. In: *Crop project: deep seismic exploration of the Central Mediterranean and Italy*, Elsevier Science and Technology 7:109–117
- Furumura T (2001) Variations in regional phase propagation in the area around Japan. *Bull Seismol Soc Am* 91:667–682
- Galadini F, Poli ME, Zanferrari A (2005) Seismogenic sources potentially responsible for earthquakes with  $M \geq 6$  in the eastern southern Alps (Thiene–Udine sector, NE Italy). *Geophys J Int* 161:739–762
- Galli MT (2005) I terremoti del gennaio del 1117. Ipotesi di un epicentro nel Cremonese, *Il Quaternario* 18:85–100
- Galli P, Castenetto S, Peronace E (2012) The MCS macroseismic survey of the Emilia 2012 earthquakes. *Ann Geophys* 55(4):663–672
- Grünthal G (1998) European Macroseismic Scale 1998 (EMS-98). European Seismological Commission, sub commission on Engineering Seismology, working Group Macroseismic Scales, Conseil de l'Europe, Cahiers du Centre Européen de Géodynamique et de Séismologie, vol 15, Luxembourg
- Herrmann RB (2013) Computer programs in seismology: an evolving tool for instruction and research. *Seismol Res Lett* 84(6):1081–1088. doi:10.1785/0220110096
- Housner GW (1952) Intensity of ground motion during strong earthquakes. Second technical report, California Institute of Technology, Pasadena, California
- Koliopoulos PK, Margaris BN, Klimis NS (1998) Duration and Energy characteristic of Greek strong motion records. *J Earthq Eng* 2(3):391–417
- Liu K-S, Tsai Y-B (2009) Large effects of Moho reflections (SmS) on peak ground motion in northwestern Taiwan. *Bull Seismol Soc Am* 99(1):255–267
- Locati M, Camassi R, Stucchi M (2011) DBMI11, la versione 2011 del Database Macrosismico Italiano. Milano, Bologna. <http://emidius.mi.ingv.it/DBMI11>
- Masi A, Vona M, Mucciarelli M (2010) Selection of natural and synthetic accelerograms for seismic vulnerability studies on RC frames. *J Struct Eng*. ASCE Special Issue devoted to Earthquake Ground Motion Selection and Modification for Nonlinear Dynamic Analysis of Structures, 137:367–378. doi:10.1061/(ASCE)ST.1943-541X.209

- Massa M, Lovati S, Sudati D, Franceschina G, Russo E, Puglia R, Ameri G, Luzi L, Pacor F, Augliera P (2012) INGV strong-motion data web-portal: a focus on the Emilia seismic sequence of May–June 2012. *Ann Geophys* 55(4):829–835
- Mele G, Rovelli A, Seber D, Barazangi M (1997) Shear wave attenuation in the lithosphere beneath Italy and surrounding regions: tectonic implications. *J Geophys Res* 102(B6):11863–11875
- Oliver J, Ewing M (1957) Higher modes of continental Rayleigh waves. *Bull Seismol Soc Am* 47:187–204
- Oliver J, Ewing M (1958) Normal modes of continental surface waves. *Bull Seismol Soc Am* 48:33–49
- Pergalani F, Romeo R, Luzi L, Petrini V, Pugliese A, Sanò T (1999) Seismic microzoning of the area struck by Umbria–Marche (Central Italy) Ms 5.9 earthquake of 26 September 1997. *Soil Dyn Earthq Eng* 18:279–296
- Piccinini D, Pino NA, Saccorotti G (2012) Source complexity of the May 20, 2012, Mw 5.9, Ferrara (Italy) event. *Ann Geophys* 55(4):569–573
- Pieri M, Groppi G (1981) Subsurface geological structure of the Po plain. CNR, Prog Final Geod, Pubbl 411, Italy
- Pondrelli S, Salimbeni S, Perfetti P, Danecsek P (2012) Quick regional centroid moment tensor solutions for the Emilia 2012 (Northern Italy) seismic sequence. *Ann Geophys* 55(4):615–621
- Riddel R (2007) On ground motion intensity indices. *Earthq Spectr* 23(1):147–173
- Rovida A, Camassi R, Gasperini P, Stucchi M (eds) (2011) CPTI11, the 2011 version of the Parametric Catalogue of Italian Earthquakes Milano, Bologna. <http://emidius.mi.ingv.it/CPTI>
- Sarò A, Peruzza L (2012) Fault-plane solutions from moment-tensor inversion and preliminary Coulomb stress analysis for the Emilia plain. *Ann Geophys* 55(4):647–654
- Somerville PG, Yoshimura J (1990) The influence of critical Moho reflections on strong ground motions recorded in San Francisco and Oakland during the 1989 Loma Prieta earthquake. *Geophys Res Lett* 17(8):1203–1206
- Stucchi M, Camassi R, Rovida A, Locati M, Ercolani E, Meletti C, Migliavacca P, Bernardini F, Azzaro R (2007) DBMI04, il database delle osservazioni macrosismiche dei terremoti italiani utilizzate per la compilazione del catalogo parametrico CPTI04. *Quaderni Geofisica* 49:1–38. Available at <http://emidius.mi.ingv.it/DBMI04/>. Accessed Apr 2011, in Italian
- Sugan M, Vuan A (2012) Evaluating the relevance of Moho reflections in accelerometric data: application to an Inland Japanese earthquake. *Bull Seismol Soc Am* 102(2):842–847
- Vuan A, Klin P, Laurenzano G, Priolo E (2011) Far-source long period displacement response spectra in the Venetian and Po plains (Italy) from 3D wavefield simulations. *Bull Seismol Soc Am* 101(3):1055–1072
- Wessel P, Smith WHF (1991) Free software helps map and display data. *Eos Trans AGU* 72(441):445–446